THE ASTROPHYSICAL JOURNAL, 560:L197–L200, 2001 October 20

SMALL-SCALE PHOTOSPHERIC FIELDS: OBSERVATIONAL EVIDENCE AND NUMERICAL SIMULATIONS

THIERRY EMONET
Astronomy and Astrophysics Center, University of Chicago, 5640 South Ellis Avenue, Chicago, IL 60637; emonet@flash.uchicago.edu
AND
FAUSTO CATTANEO
Department of Mathematics, University of Chicago, 5734 South University Avenue, Chicago, IL 60637; cattaneo@flash.uchicago.edu
Received 2001 August 1; accepted 2001 September 7; published 2001 September 26

ABSTRACT

Observations suggest that magnetic fields at the solar photosphere may be structured below the limit of the present resolution. We argue that numerical simulations could be used in a complementary way to observations in order to study the small-scale structure of photospheric fields. We present a number of illustrative examples.

Subject headings: convection — MHD — Sun: magnetic fields — Sun: photosphere

1. INTRODUCTION

Standard solar magnetic field measurements based on the ordinary Zeeman effect suggest that the quiet Sun is mainly field-free with magnetic flux concentrated into small isolated areas with an average filling factor of 1% (see, e.g., Stenflo 1994). These observations are limited by the difficulty of resolving weak magnetic structures ($\lesssim$50 G) and by the cancellation of opposite polarities within the resolution elements (the best resolutions currently are $0\farcs2 \approx 150$ km).

New observational techniques with higher sensitivity to weak magnetic fields are changing this concept of a mainly field-free quiet Sun. The best examples are perhaps the recent measurements using the Hanle depolarization effect. Compared to Zeeman splitting, the Hanle effect is sensitive only to weak magnetic strengths ($\lesssim$50 G) and does not suffer from the cancellation of opposite polarities; i.e., it measures the *unsigned* magnetic intensity (Stenflo 1999). Thus, the Hanle and Zeeman effects are complementary and, used together, provide for the first time a nearly complete picture of the spectrum of magnetic intensities in the quiet Sun. The most recent observations of this kind suggest that the photosphere is permeated by randomly oriented magnetic fields of intensity between 4 and 40 G (Stenflo, Keller, & Gandorfer 1998). Lin & Rimmele (1999) partially confirm these results by measuring Zeeman splitting in highly sensitive infrared lines and conclude that some 68% of the so-called quiet Sun actually contains weak magnetic fields.

There is other indirect evidence for the existence of a fine-scale structuring of magnetic fields in the photosphere: observed asymmetries in Stokes profiles can be reproduced in a uniform way by assuming the existence of magnetic structures with characteristic sizes smaller than the mean free path of a photon along the line of sight. An elegant implementation of this idea is the microstructured magnetic atmosphere (MISMA) hypothesis used for the diagnostic of "turbulent" fields with the Zeeman effect (Sánchez Almeida & Lites 2000 and references therein).

High-resolution observations with high temporal cadence also provide information about the dynamics of the magnetic concentrations ($\gtrsim$50 G) and give some hints about their origin. With high resolution ($0\farcs2$), Berger & Title (1996) and Berger et al. (1998) observe the evolution of magnetic bright points in active region plages. These magnetic features appear to be in a highly dynamic state, undergoing significant morphological changes on timescales on the order of 100 s or less. The authors conclude that these magnetic concentrations are not consistent with the concept of stable (or even oscillating) flux tubes. Instead, it seems that flux located within a particular element at a given time is redistributed to other elements within a turnover time. Similar conclusions are reached by Lin & Rimmele (1999), who observe magnetic features with mixed polarities in the quiet Sun. With lower resolution but without degradation due to the seeing, Schrijver et al. (1997) observe the evolution of magnetic features in time series of the Michelson Doppler Imager magnetograms. They conclude that the quiet mixed-polarity network is generated locally.

A number of theoretical studies have suggested that a substantial fraction of the magnetic flux present in quiet photospheric regions could be generated locally (Meneguzzi & Pouquet 1989; Durney, De Young, & Roxburgh 1993; Petrovay & Szakaly 1993; Cattaneo 1999). The starting point for these studies is the result from fast dynamo theory that any three-dimensional chaotic flow with a high Reynolds number is likely to be a dynamo (Vainshtein & Kichatinov 1986). Direct numerical simulations by Cattaneo (1999) support this possibility and show that thermally driven turbulent convection can generate and maintain a sizable amount of magnetic energy.

The picture that emerges is that magnetic fields in the quiet Sun and plages are highly spatially intermittent with a weak mean and strong fluctuations and with individual elements that have structuring down to scales smaller than the resolution cutoff. The spectrum of magnetic intensities seems to be continuous with weak fields filling most of the volume and strong magnetic concentrations having a filling factor of a few percent only.

The question naturally arises how best to study this small-scale structure of magnetic fields at the solar photosphere. Order-of-magnitude estimates of the magnetic Reynolds number at the surface of the convection zone suggest that the magnetic field should be structured down to spatial scales on the order of a few kilometers (Stix 1989). This is far smaller than the best resolution achieved with today's observations (~150 km). Moreover, it is difficult in general to resolve scales smaller than the mean free path of a photon (50–100 km).

One interesting possibility may be offered by direct numerical simulations. It is now possible to run such simulations for physically relevant configurations with an effective numerical resolution higher than that of the observations. The results of these simulations could provide the starting point for a critical discussion of the properties of photospheric magnetic fields on observationally unresolved scales. We illustrate the potential of this

approach by analyzing some of the data sets generated by high-resolution simulations of convectively driven magnetoturbulence (Cattaneo 1999; Emonet, Cattaneo, & Weiss 2001; F. Cattaneo, T. Emonet, & N. O. Weiss 2001, in preparation). We should point out that these results were obtained from a greatly idealized model based on the Boussinesq approximation and do not include such physically important processes as ionization, compressibility, and radiative transfer. On the other hand, they do provide an accurate description of the interaction between magnetic fields and convection in a strongly turbulent regime.

We consider situations in which the magnetic field is generated entirely by the convective turbulence (dynamo action) as well as situations in which a vertical magnetic field is externally imposed. In order to mimic a variety of solar conditions, quiet Sun, plages, active regions, we consider cases where the imposed field varies from zero (dynamo) to values high enough substantially to modify the convective flow (magnetoconvection).

Section 2 contains a description of the data set. Next, we analyze the preferred structure of magnetic fields as a function of the externally imposed magnetic field strength (§ 3). Finally, we study the effects of limited resolution on observations of small-scale magnetic fields (§ 4).

2. DATA SET DESCRIPTION

The data set is generated by simulating a three-dimensional, thermally driven convection in a plane-parallel layer of incompressible (Boussinesq) fluid with constant kinematic viscosity ν, thermal diffusivity κ, and magnetic diffusivity η. The boundary conditions are periodic in the two horizontal directions, and in the vertical direction they correspond to impenetrable stress-free boundaries on which the temperature is kept constant and the horizontal component of the magnetic field vanishes (see Cattaneo 1999 and Emonet et al. 2001 for more details). All simulations have the following dimensionless parameters: aspect ratio $10 \times 10 \times 1$, Rayleigh number 5×10^5, and Prandtl numbers $\nu/\kappa = 1$ and $\nu/\eta = 5$. The typical resolution is $512 \times 512 \times 97$ collocation points. All the runs are started by adding to a fully convective state either a random magnetic seed field (dynamo case) or a uniform vertical magnetic field of intensity B_0. We compare results from five cases (0–4) obtained by setting $B_0 = 0$ (dynamo), 25, 50, $50\sqrt{2}$, and 100 (in units of the Alfvén speed). For comparison, the equipartition strength in the dynamo solution is $B_{\rm eq} = 200$.

To get a feel for the relative magnitude of these values, we translate them into "solar" values by assuming an equipartition field strength at the photosphere of 400 G. Then these become 0, 50, 100, $100\sqrt{2}$, and 200 G. Depending on the prescribed vertical flux, the system settles into different regimes. For very small values of B_0, the turbulence dominates the dynamics, and magnetic energy is generated by dynamo action. For moderate values of B_0, the convective flow is modified by the magnetic field. The horizontal size of the convection cells are smaller (Fig. 1). In the rest of the Letter, we concentrate on the structure of the solutions in the upper thermal boundary layer, i.e., the region where there are substantial deviations from a mean isothermal atmosphere (approximately the top 10% of the layer in these simulations).

3. SURFACE APPEARANCE

Gray-scale plots in a horizontal plane near the surface of the computational domain provide information about the global spatial distribution of the solution. The temperature fluctuations and the vertical component of the magnetic field are shown in Figure 1 for cases 0 and 4. Strong magnetic fluctuations are found preferentially near regions of strong downflows located in between the convective cells. Their polarities are *mixed* in the dynamo case. In the interior of the cells, the magnetic field is weak but *not zero*. Adding a vertical magnetic field can lead to modification of the convective flow. The horizontal scale of the cells gradually diminishes, and, as B_0 is increased, the intergranular lanes become wider.

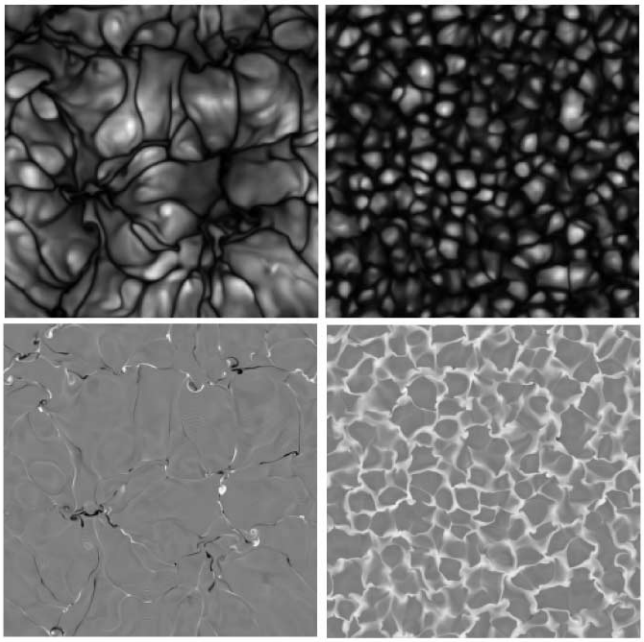

FIG. 1.—Gray-scale plots of the temperature fluctuations (*top panels*) and the vertical component of the magnetic field (*bottom panels*) in a horizontal plane located 2 grid points below the surface of the computational domain for a dynamo (case 0, *left panels*) and a magnetoconvective case (case 4, *right panels*). The net magnetic flux is zero on the left and positive on the right. The filling factor of strong magnetic features ($>2B_{\rm eq}$) is 0.3% on the left and 3% on the right (see Fig. 2).

3.1. *Weak and Strong Magnetic Components*

Insights into the distributions of weak and strong magnetic features can be grasped by measuring the probability density function (PDF) of the (signed) magnetic intensity or, in other words, the probability of finding a fluid parcel with a magnetic intensity between $b = B\,\mathrm{sign}\,(B_z)$ and $b + db$ (the top two panels in Fig. 2). The PDFs have their maxima near small values of B, even when a moderate net magnetic flux is added to the system. Thus, weak magnetic fields fill most of the volume. The filling factor of weak fields ($B < B_{\rm eq}$) is 97% in the dynamo case and gradually decreases to 77% as B_0 is increased up to 100 (the bottom panels in Fig. 2).

The PDFs plotted in Figure 2 tend to have an exponential shape (especially in the dynamo case) for which the probability of very weak and very strong fluctuations is higher than if the magnetic field was simply redistributed by a random process with a Gaussian signature. As a result, the magnetic field is highly intermittent, and strong magnetic features as intense as 2–4 times equipartition are routinely generated by the dynamo. Their filling factor is small though: 0.3% for intensities higher than $2B_{\rm eq}$. We note, however, that these magnetic concentrations are generated irrespective of compressibility. When a net magnetic flux is added to the system, an additional hump appears on the right-hand side of the PDF (the right panels in Fig. 2).

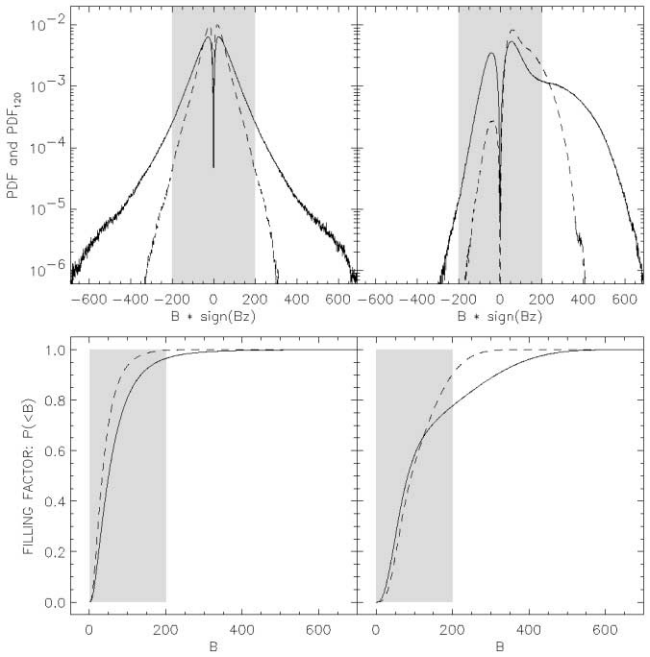

FIG. 2.—*Top panels*: PDFs of $B\,\mathrm{sign}\,(B_z)$ in the upper thermal boundary layer (10 grid planes) for cases 0 and 4. *Bottom panels*: Filling factors of magnetic fields with intensities smaller than B. The gray shading indicates regions where $B < B_{eq} = 200$. The dashed lines indicate the effect of limiting the resolution of the data by convoluting it with a Gaussian filter (FWHM = 12 pixels ≈120 km).

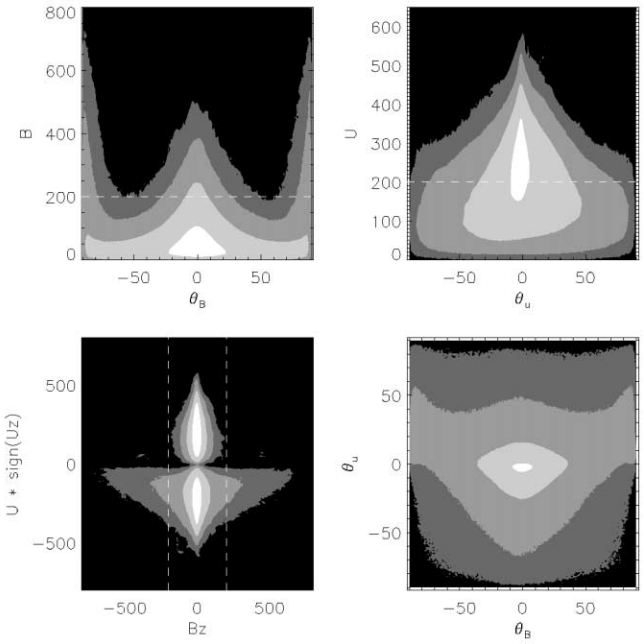

FIG. 3.—Joint PDFs for (θ_B, B), (θ_u, u), (B_z, u_z), and (θ_B, θ_u) in the upper thermal boundary layer. The six shadings correspond to a logarithmic scale with values larger than 10^{-3} in white and smaller than 10^{-6} in black. The dashed lines represent the equipartition level.

Its Gaussian shape suggests that the process of intensification of the mean field is different from the generation of the magnetic field by dynamo action.

3.2. *Time Evolution*

The magnetic field evolves in close relation with the convection cells. A careful study of time sequences of the magnetic distribution near the surface and in the interior reveals that the turbulent flow is constantly destroying and generating the magnetic field. The magnetic field that appears in the bulk of the convective layer is transported toward the boundaries by the convective cells. When it comes close to the surface, it is pushed toward the border of the cells, eventually ending up in the cellular corners where it is wrapped and stretched by swirling downflows. The lifetime of any magnetic flux present in downflowing regions is on the order of *one* overturning time. By this we mean that if the process of generation and advection of new flux into a cellular corner were interrupted, it would take approximately one turnover time to deplete the magnetic flux at a downflow site. This should be contrasted with the relatively long lifetime of certain regions of strong downflow—*several* turnover times. These, in particular, can lead to the persistence of a magnetic *pattern*. However, the lifetime of the pattern should not be identified with the much shorter lifetime of the individual flux elements.

3.3. *Spatial Correlations between* $\boldsymbol{B}$ *and* $\boldsymbol{u}$

The instantaneous magnetic configuration in the upper layers can be further studied using joint PDFs. Joint PDFs for (θ_B, B), (θ_u, u), (B_z, u_z), and (θ_B, θ_u), where θ_B, θ_u are the angles between $\boldsymbol{B}$, the velocity $\boldsymbol{u}$, and the horizontal direction, are plotted in Figure 3 for case 0. The top left panel shows that the strongest magnetic fields are vertical, whereas weaker and very weak magnetic features tend to be horizontal. The high probability of finding horizontal fields is a natural consequence of the structure of the flow close to the boundary; as shown in the top right panel, most of the volume near the surface is occupied by vigorous *horizontal* flows. The orientation of the velocity (θ_u) is random for small speeds ($\lesssim$50). The bottom panels in Figure 3 show the correlations between $\boldsymbol{u}$ and $\boldsymbol{B}$. The bottom left panel indicates that strong *vertical* magnetic features ($>2B_{eq}$) only exist within downdrafts. The amplitude of the velocity within downdrafts, however, diminishes to zero when B_z becomes very strong. Finally, the bottom right panel in Figure 3 shows that near the surface, both $\boldsymbol{u}$ and $\boldsymbol{B}$ are preferentially horizontal. But there is a clear difference between upflows and downflows. In the upflows, the magnetic field is randomly oriented, whereas when θ_u is negative, and especially when it approaches $-90°$, the magnetic and velocity fields become more and more aligned.

We note that the detailed structure of the joint PDFs depends to a large extend on our particular choice of boundary conditions (Thelen & Cattaneo 2000). Nevertheless, similar techniques could be used to gather useful information in more realistic cases.

4. EFFECTS OF LIMITED RESOLUTION

If we assume that the typical horizontal size of one granule in the quiet Sun is about 1000 km, then the smallest numerically resolved features in the solutions are approximately 30 km. Since the best resolution achieved with current telescopes is about 150 km, the present data can be used to study the effects of limited resolution on observations. One can simply convolute the fully resolved solutions with a Gaussian filter of given width (FWHM = 12 grid points ≈120 km) and compare the statistics of the coarse-grained data set with the statistics of the original set.

The difference between the resolved and coarse-grained data

is apparent in Figure 4, which shows the coarse-grained data corresponding to the bottom left panel in Figure 1. The fine spatial structure is lost; mixed polarities clearly visible near the downdrafts in the original data have been replaced with uniform fields. Thus, some substantial amount of magnetic flux is canceled by the lack of resolution. The right panel in Figure 4 shows the magnetic flux density as a function of the width of the resolution element in a horizontal plane near the surface for case 0. At 1″ resolution, *about 90% of the flux density is canceled*. The comparison between the original PDFs and the one for the coarse-grained data (the dashed curves in Fig. 2) gives some idea of which part of the information is mostly affected by the lack of resolution. In all cases, the wings of the PDF disappear first. In other words, the lack of resolution tends to eliminate the (stretched) exponential behavior from the profiles (the signature of the dynamo action) in favor of a more Gaussian appearance.

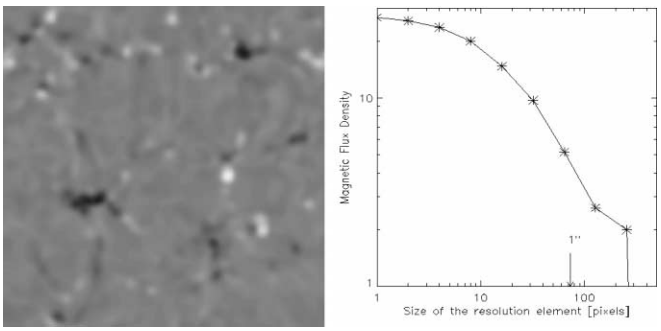

FIG. 4.—The left panel shows the effect of coarse-graining. The data are the same as in the bottom left panel of Fig. 1. The graph in the right panel shows the magnetic flux density as a function of the width of the resolution element for a plane located near the surface in the dynamo solution.

5. CONCLUSION

Many of the properties of magnetic fields at the visible photosphere are shared by high-resolution numerical simulations of the interaction between magnetic fields and turbulent convection. In particular, the existence of a highly intermittent magnetic field with weak mean everywhere is in agreement with recent observations of weak magnetic fields and with the MISMA hypothesis. The continous generation and transport toward long-lived downflowing regions of strong magnetic fluctuations is in accordance with observations by Berger & Title (1996), Berger et al. (1998), and Lin & Rimmele (1999) and with the inconsistency between their observations and the concept of a stable isolated subarcsecond flux tube.

The above considerations indicate that numerical simulations can be a useful tool for studying small-scale photospheric fields. Their ability to probe scales that are below the limit of resolution make them complementary to direct observations. We anticipate that in the future, simulations will be used to study the effects of limited resolution on direct observations or to construct averaged quantities that are measurable at the current observational resolution.

The numerical solutions presented here are based on a highly idealized model. More realistic models that include, for instance, the effects of compressibility, ionization, radiative transfer, or more sophisticated boundary conditions can probably also be constructed. We hope that the considerations of the present Letter will lead toward their development.

This work was partially supported by the NASA SR&T and HPCC Initiatives and by the Department of Energy ASCI Initiative at the University of Chicago.

REFERENCES

Berger, T. E., Löfdahl, M. G., Shine, R. A., & Title, A. M. 1998, ApJ, 506, 439
Berger, T. E., & Title, A. M. 1996, ApJ, 463, 365
Cattaneo, F. 1999, ApJ, 515, L39
Durney, B. R., De Young, D. S., & Roxburgh, I. W. 1993, Sol. Phys., 145, 207
Emonet, T., Cattaneo, F., & Weiss, N. O. 2001, in Dynamo and Dynamics: A Mathematical Challenge, ed. P. Chossat, D. Armbruster, & J. Oprea (Dordrecht: Kluwer), 173
Lin, H., & Rimmele, T. 1999, ApJ, 514, 448
Meneguzzi, M., & Pouquet, A. 1989, J. Fluid Mech., 205, 297
Petrovay, K., & Szakaly, G. 1993, A&A, 274, 543
Sánchez Almeida, J., & Lites, B. W. 2000, ApJ, 532, 1215
Schrijver, C. J., Title, A. M., van Ballegooijen, A. A., Hagenaar, H. J., & Shine, R. A. 1997, ApJ, 487, 424
Stenflo, J. O. 1994, Solar Magnetic Fields: Polarized Radiation Diagnostics (Dordrecht: Kluwer)
———. 1999, in Solar Polarization, ed. K. N. Nagendra & J. O. Stenflo (Dordrecht: Kluwer), 1
Stenflo, J. O., Keller, C. U., & Gandorfer, A. 1998, A&A, 329, 319
Stix, M. 1989, The Sun: An Introduction (New York: Springer)
Thelen, J.-C., & Cattaneo, F. 2000, MNRAS, 315, L13
Vainshtein, S. I., & Kichatinov, L. L. 1986, J. Fluid Mech., 168, 73